BEHAVIOR OF SINGLET OXYGEN IN THE OXYGEN–IODINE TRANSFER LASER†

R. F. HEIDNER III

Aerophysics Laboratory, The Aerospace Corporation, Los Angeles, CA 90009 (U.S.A.)

(Received January 24, 1984)

Summary

The kinetic processes that affect the decay of $O_2(^1\Delta)$ in the oxygen–iodine transfer laser are discussed. The kinetics of O_2^* removal in the absence of iodine are now quite well established. A brief review of this topic is presented.

When I_2 is added to O_2^*, a distinction can be made between the behavior of O_2^* when both I_2 and I are present, and when I_2 is fully dissociated into atoms. In the latter case, energy pooling between $O_2(^1\Delta)$ and I^* is the dominant process unless a strong I^* quencher (*e.g.* H_2O) is present. In the former case, the $O_2(^1\Delta)$-driven chain reaction mechanism for I_2 dissociation is the dominant feature of the kinetics. A detailed description of each of these regimes is critical to the understanding of the oxygen–iodine laser.

1. Introduction

The chemical oxygen–iodine laser (COIL) [1 - 3] is based on transferring energy from a *majority* energy storage species ($O_2(^1\Delta)$) to a *minority* receptor species ($I(^2P_{3/2})$):

$$O_2(^1\Delta) + I(^2P_{3/2}) \underset{k_{-1}}{\overset{k_1}{\longleftrightarrow}} O_2(^3\Sigma) + I(^2P_{1/2}) \quad (1)$$

$K_{EQ} = k_1/k_{-1} = 2.9$ at $T = 295$ K. An energy level diagram for the low-lying electronic states of O_2, I_2 and I is shown in Fig. 1. Examination of the above electronic state equilibrium and the threshold criterion for the atomic iodine laser ($[I^*]/[I] > 0.5$) yields the conclusion that $[O_2(^1\Delta)]/[O_2(^3\Sigma)] > 0.17$ in order to sustain continuous wave laser oscillation. While the yield of $O_2(^1\Delta)$ from the reaction of Cl_2 and basic hydrogen peroxide is extremely high, deactivation of $O_2(^1\Delta)$ to $O_2(^3\Sigma)$ quickly degrades the extractable energy from such a device.

†Paper presented at the COSMO 84 Conference on Singlet Molecular Oxygen, Clearwater Beach, FL, U.S.A., January 4 - 7, 1984.

0047-2670/84/$3.00

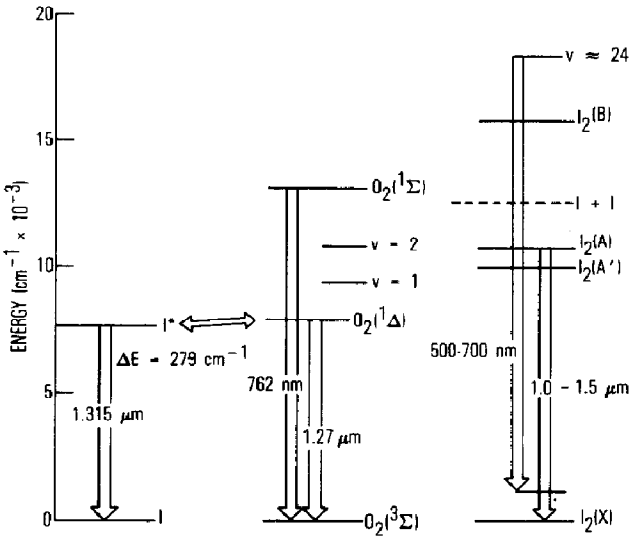

Fig. 1. Low-lying electronic energy levels and observed spectral emissions for O_2, I_2 and I.

Direct quenching of $O_2(^1\Delta)$ is extremely deleterious to laser performance; fortunately most $O_2(^1\Delta)$ quenching processes are extremely inefficient. Quenching of I* is important because process (1) connects the $O_2(^1\Delta)$ energy storage reservoir with the I* lasing medium. I* quenching processes become significant loss mechanisms for $O_2(^1\Delta)$ at high $[I^*]/[O_2(^1\Delta)]$ ratios.

In the review to follow, we shall pay particular attention to the mechanism by which O_2^* dissociates molecular I_2 (k_2) and to the second-order energy pooling (k_{3a}) and electronic quenching (k_{3b}, k_{3c} and k_{3d}) processes:

$$nO_2^* + I_2 \xrightarrow{k_2} nO_2 + 2I \tag{2}$$

$$O_2(^1\Delta) + I^* \xrightarrow{k_{3a}} O_2(^1\Sigma) + I \tag{3a}$$

$$O_2(^1\Delta) + I^* \xrightarrow{k_{3b}} O_2(^3\Sigma) + I \tag{3b}$$

$$O_2(^1\Delta) + I^* \xrightarrow{k_{3c}} O_2(^1\Delta) + I \tag{3c}$$

$$O_2(^1\Delta) + I^* \xrightarrow{k_{3d}} O_2(^3\Sigma) + I^* \tag{3d}$$

In the "conventional" COIL device, these processes are intrinsic loss processes for $O_2(^1\Delta)$ that must be tolerated. Finally, we shall briefly examine the advantages of replacing I_2 by an alternative I precursor that is "pre-mixable" with $O_2(^1\Delta)$.

2. Experimental details

The work reported from our laboratory has been performed on two different experimental systems. The kinetic flow tube apparatus (Fig. 2) has been described in great detail in ref. 4. The excimer laser photolysis apparatus (Fig. 3) has been described in ref. 5. In both cases, O_2^* is created by a microwave discharge in pure O_2 ($[O_2(^1\Delta)]/[O_2(^3\Sigma)] < 0.1$) and the $O(^3P)$ atoms are removed on a heated HgO surface just downstream of the discharge.

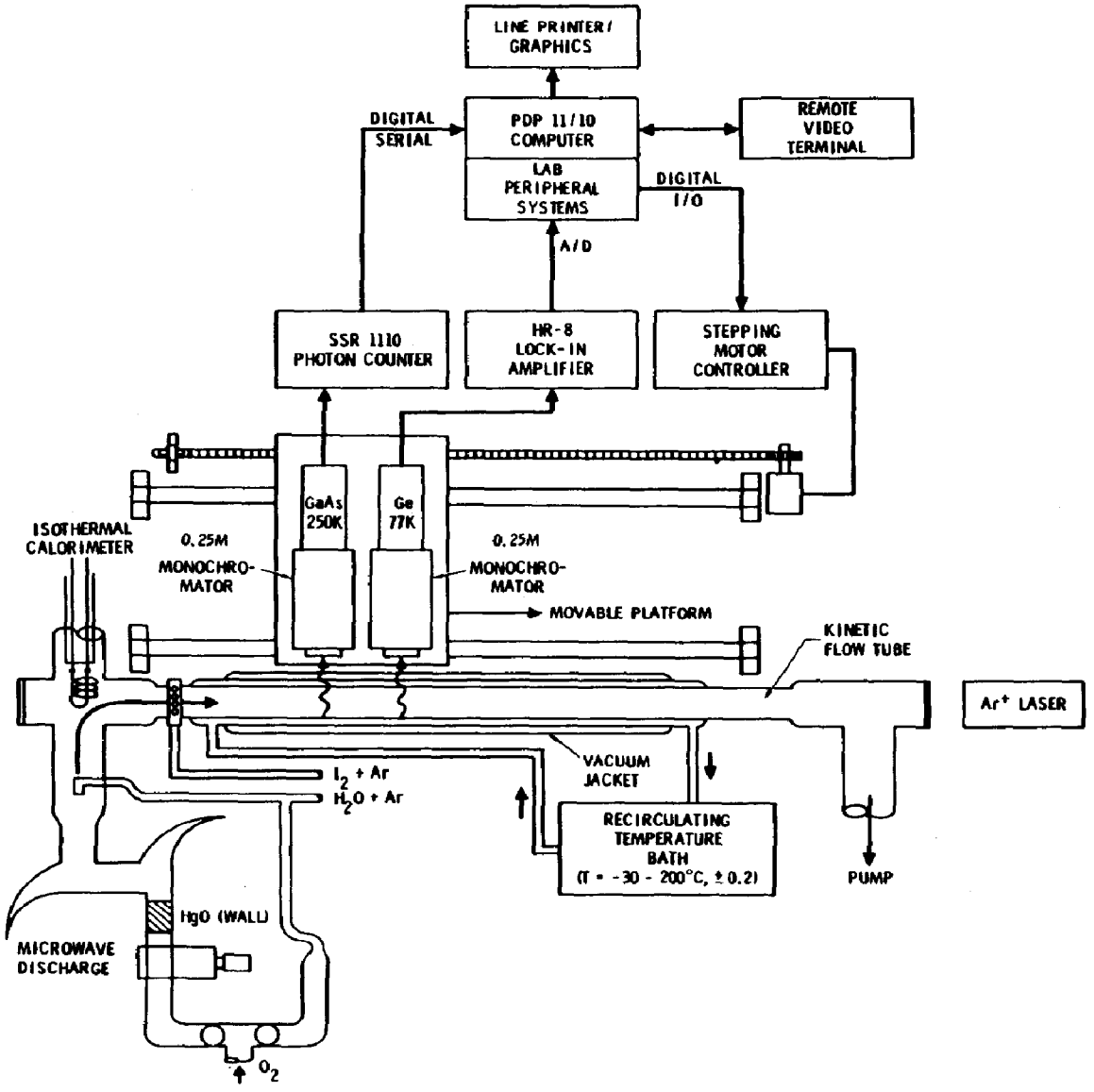

Fig. 2. Schematic diagram of the computer-controlled kinetic flow tube apparatus.

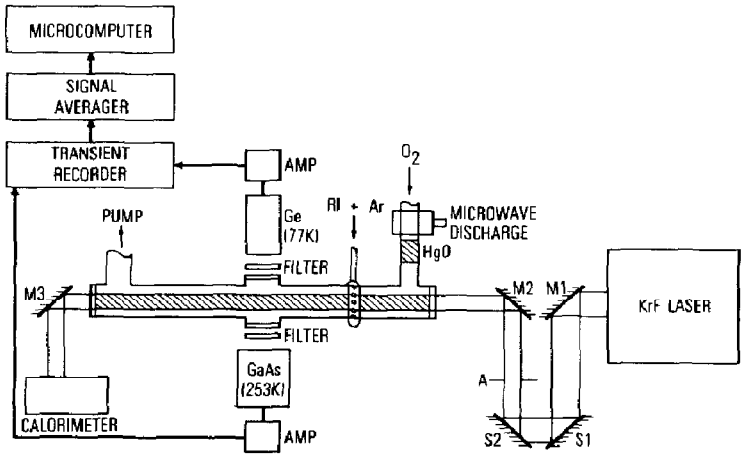

Fig. 3. Schematic diagram of the excimer photolysis flow tube apparatus.

Although the apparatus in Fig. 3 is a flow system, the time histories of the important densities are monitored by time-resolved emission spectroscopy following the excimer laser photolysis pulse. In the apparatus of Fig. 2, steady state emission intensities are monitored as a function of distance down the flow tube in order to extract kinetic information. In each case, $[O_2(^1\Delta)]$ is calibrated absolutely by isothermal calorimetry and $[I^*]$ is related to it by the ratio of the Einstein coefficients. Concentrations of $O_2(^1\Sigma)$, $I_2(A\,^3\Pi_{1u})$ and $I_2(B\,^3\Pi_{0^+})$ were also followed during some experiments. Two experimental details are worth emphasizing. First, the treatment of the walls in the flow tube apparatus is critical to the results obtained. The walls in our apparatus were coated with a low melting halogenated wax (Halocarbon Inc.) that was very inefficient at recombining iodine atoms. Secondly, the use of an extremely sensitive intrinsic germanium detector (ADC 403 HS) permitted the detection of $O_2(^1\Delta)$ and I^* in the flow tube with an excellent signal-to-noise ratio and I^* with good time response in the excimer photolysis apparatus.

3. Results and analysis

3.1. Decay of $O_2(^1\Delta)$ in the absence of I_2 and I

The decay of $O_2(^1\Delta)$ can be accurately described by a combined first- and second-order decay equation based on the following processes:

$$O_2(^1\Delta) + O_2(^1\Delta) \xrightarrow{k_{4a}} O_2(^1\Sigma) + O_2(^3\Sigma) \tag{4a}$$

$$O_2(^1\Delta) + O_2(^1\Delta) \xrightarrow{k_{4b}} O_2(^1\Delta) + O_2(^3\Sigma) \tag{4b}$$

$$O_2(^1\Delta) + O_2(^1\Delta) \xrightarrow{k_{4c}} O_2(^3\Sigma) + O_2(^3\Sigma) \tag{4c}$$

$$O_2(^1\Sigma) + M \xrightarrow{k_{5a}} O_2(^1\Delta) + M \quad (5a)$$

$$O_2(^1\Sigma) + M \xrightarrow{k_{5b}} O_2(^3\Sigma) + M \quad (5b)$$

$$O_2(^1\Sigma) + \text{wall} \xrightarrow{k_{6a}} O_2(^1\Delta) + \text{wall} \quad (6a)$$

$$O_2(^1\Sigma) + \text{wall} \xrightarrow{k_{6b}} O_2(^3\Sigma) + \text{wall} \quad (6b)$$

$$O_2(^1\Delta) + M \xrightarrow{k_7} O_2(^3\Sigma) + M \quad (7)$$

$$O_2(^1\Delta) + \text{wall} \xrightarrow{k_8} O_2(^3\Sigma) + \text{wall} \quad (8)$$

The solution can be written as follows:

$$[O_2(^1\Delta)]^{-1} = \left\{ [O_2(^1\Delta)]_0^{-1} + \frac{A}{B} \right\} \exp(Bt) - \frac{A}{B} \quad (9)$$

where

$$A = 2k_{4a} - \frac{k_{4a}(k_{5a} + k_{6a})}{k_5 + k_6} + k_{4b} + 2k_{4c}$$

and

$$B = k_8 + k_7^{M}[M]$$

Making the assumption that $O_2(^1\Sigma)$ is quenched predominantly to $O_2(^1\Delta)$ and that the two dominant quenchers from a COIL chemical generator are $O_2(^3\Sigma)$ and H_2O, we can write

$$A = k_{4a} + k_{4b} + 2k_{4c}$$

$$B = k_8 + k_7^{O_2}[O_2(^3\Sigma)] + k_7^{H_2O}[H_2O]$$

Table 1 contains the necessary rate coefficient information for evaluating $O_2(^1\Delta)$ decays under these conditions. Because the rate coefficient k_4 is so small, it is extremely difficult to detect the second-order decay component in a pure O_2 or an $O_2 + H_2O$ system.

3.2. Decay of $O_2(^1\Delta)$ in the presence of I and I ($[I_2] = 0$)*

3.2.1. Decay curves for $[O_2(^1\Delta)] \gg [O_2(^3\Sigma)]$

Under conditions that are approachable with a chemical generator for $O_2(^1\Delta)$, the relationship between $O_2(^1\Delta)$ and I* can be written as follows [4]:

$$[I^*] = \frac{2X[I_2]_0}{1 + X} \quad (10)$$

TABLE 1

Rate coefficient data for $O_2(^1\Delta)$ quenching in pure O_2 (T = 295 K)

Process	*M*	*Rate coefficient* (cm^3 $molecule^{-1}$ s^{-1})	*Reference*
k_{4a}		$(2.0 \pm 0.5) \times 10^{-17}$	[6]
		$(2.0 \pm 0.6) \times 10^{-17}$	[8]
k_4		$< 5 \times 10^{-17}$	[7]
k_5	O_2	$(4.0 \pm 0.4) \times 10^{-17}$	[9]
		$(3.9 \pm 0.2) \times 10^{-17}$	[10]
	H_2O	$(5 \pm 1) \times 10^{-12}$	[11]
		4.7×10^{-12}	[12]
		$(6.7 \pm 0.5) \times 10^{-12}$	[13]
k_6		$\gamma = 1 \times 10^{-2}$ (Pyrex)	[6]
		2×10^{-2} (Pyrex)	[8]
		1×10^{-3} (Halocarbon)	[8]
k_7	O_2	$(1.6 \pm 0.05) \times 10^{-18}$	[14]
		$(1.5 \pm 0.05) \times 10^{-18}$	[15]
	H_2O	$(4 \pm 1) \times 10^{-18}$	[11]
k_8		$\gamma = 2 \times 10^{-5}$ (Pyrex)	[6]
		1.2×10^{-5} (Pyrex)	[14]
		3×10^{-5} (Halocarbon)	[8]

γ represents the wall recombination probability: $\gamma = 2Rk/c$ in a cylindrical flow tube, where c is the oxygen mean velocity, R is the tube radius and k (s^{-1}) is the measured removal rate.

where $X = K_{EQ}[O_2(^1\Delta)]/[O_2(^3\Sigma)] = [I^*]/[I]$. In this case, since $X \gg 1$, $[I^*] = 2[I_2]_0$, *i.e.* all the iodine atoms are in the excited state. Thus, $[I^*]$ can be treated as one of the constant quenchers in eqn. (7).

3.2.2. Decay curves for $[O_2(^1\Delta)] = (0.1 - 1.0)[O_2(^3\Sigma)]$

In this important region for the chemical laser, analytic modeling is complicated and numerical methods are to be preferred.

3.2.3. Decay curves for $[O_2(^1\Delta)] < 0.1[O_2(^3\Sigma)]$

In this regime where flow tube experiments employing microwave discharge production of O_2^* operate, eqn. (10) reduces to

$$[I^*] = \frac{2K_{EQ}[O_2(^1\Delta)][I_2]_0}{[O_2]_{tot} + 1.9[O_2(^1\Delta)]} \approx C'[O_2(^1\Delta)] \tag{11}$$

where $[I^*]$ is directly proportional to $O_2(^1\Delta)$. For this last case, we can write an $O_2(^1\Delta)$ decay equation analogous to eqn. (9) based on an analysis originally put forth by Derwent and Thrush [16]:

$$[O_2(^1\Delta)]^{-1} = \left\{ [O_2(^1\Delta)]_0^{-1} + \frac{C}{D} \right\} \exp(Dt) - \frac{C}{D} \tag{12}$$

where

$$C = A + \frac{k_1}{k_{-1} + k_{13}} (k_{3a} + 2k_{3b} + k_{3c} + k_{3d}) \frac{[I]}{[O_2(^3\Sigma)]}$$

$$= A + K_{EQ}(k_{3a} + 2k_{3b} + k_{3c} + k_{3d}) \frac{[I]}{[O_2(^3\Sigma)]}$$

and

$$D = B + \left\{ k_{14} + \frac{k_{13}k_1 + k_1(k_{15}^{M}[M] + k_{16} + k_{17})/[O_2(^3\Sigma)]}{k_{-1} + k_{13}} \right\} [I]$$

$$D = B + \left\{ k_{14} + K_{EQ}\left(k_{13} + \frac{k_{15}^{M}[M] + k_{16} + k_{17}}{[O_2(^3\Sigma)]} \right) \right\} [I]$$

$$= B + \left\{ k_{eff} + \frac{K_{EQ}(k_{15}^{M}[M] + k_{16} + k_{17})}{[O_2(^3\Sigma)]} \right\} [I]$$

$$k_{eff} = k_{14} + K_{EQ}k_{13}$$

The terms A and B were defined in eqn. (9). The term k_{eff} was introduced by Derwent and Thrush [16] and has been used subsequently by other researchers [8] to analyze their data. The additional processes introduced above are defined as follows:

$$I^* + O_2(^3\Sigma) \xrightarrow{k_{13}} I + O_2(^3\Sigma) \tag{13}$$

$$O_2(^1\Delta) + I \xrightarrow{k_{14}} O_2(^3\Sigma) + I \tag{14}$$

$$I^* + M \xrightarrow{k_{15}} I + M \tag{15}$$

$$I^* + \text{wall} \xrightarrow{k_{16}} I + \text{wall} \tag{16}$$

$$I^* \xrightarrow{k_{17}} I + h\nu \tag{17}$$

We shall show that $k_{-1} \gg k_{13}$ allowing K_{EQ} to replace the term $k_1/(k_{-1} + k_{13})$ in the definitions of C and D above. Figure 4, taken from ref. 17, shows that with H_2O as an I^* quencher a regime is qualitatively observed where first- and second-order components are both significant ($[H_2O] = 0$). On addition of H_2O, single-exponential decays begin to appear. As noted in ref. 17, the

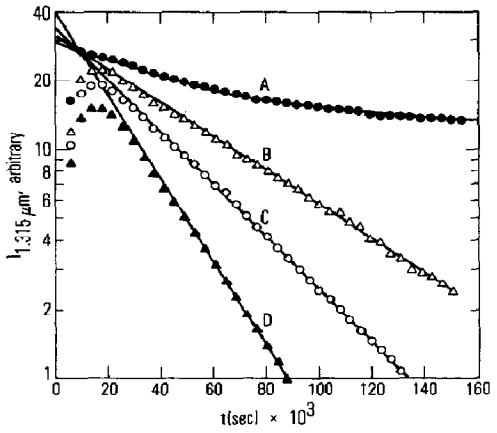

Fig. 4. I* decay profiles as a function of $[H_2O]$ (these profiles mimic $[O_2(^1\Delta)]$ decay) (P = 3.15 Torr; $[O_2(^1\Delta)]_0 = 6.5 \times 10^{15}$ molecules cm^{-3}; $[O_2(^3\Sigma)]_0 = 7.4 \times 10^{16}$ molecules cm^{-3}; $[I_2]_0 = 7.1 \times 10^{13}$ molecules cm^{-3}; balance, argon): curve A, $[H_2O]$ = 0 molecules cm^{-3}; curve B, $[H_2O] = 1.0 \times 10^{15}$ molecules cm^{-3}; curve C, $[H_2O] = 2.1 \times 10^{15}$ molecules cm^{-3}; curve D, $[H_2O] = 4.1 \times 10^{15}$ molecules cm^{-3}.

derived value of $k_{15}{}^{M} = 1.7 \times 10^{-12}$ cm^3 $molecule^{-1}$ s^{-1} is in good agreement with literature values (Table 2).

As is typical for combined first- and second-order decays, an unambiguous deconvolution is very difficult without exceedingly precise data. This system is no exception to that rule. Derwent and Thrush [16] concluded that the second-order component of the $O_2(^1\Delta)$ decay in the presence of I* was not observable; however, our studies are not consistent with that conclusion.

In Fig. 5(a), we see an $O_2(^1\Delta)$ decay *versus* time curve taken in our kinetic flow tube. A two-parameter non-linear least-squares fit to these data is superimposed. Figure 5(b) shows the data plotted as though they represent a pure second-order decay. The first-order wall decay (measured *without* I) is exceedingly small and, clearly, the incremental first-order decay component in the presence of I and I* is small as well. It should be noted that the relative $[O_2(^1\Delta)]$ must be determined by obtaining a difference spectrum since $I_2(A\,^3\Pi_{1u} \rightarrow X\,^1\Sigma)$ emission overlaps the $O_2(a\,^1\Delta \rightarrow X\,^3\Sigma)$ emission band. Analysis of the C and D coefficients in eqn. (12) as a function of $[I]/[O_2(^3\Sigma)]$ gives the plot in Fig. 6. From it, we estimate that $k_{3a} + 2k_{3b} + k_{3c} + k_{3d} = 2.1 \times 10^{-13}$ cm^3 $molecule^{-1}$ s^{-1}. The rate coefficient k_{3a} has been measured to be about 1×10^{-13} cm^3 $molecule^{-1}$ s^{-1} (Table 2). On addition of I_2, we find that the increase in the first-order decay coefficient, *i.e.* $D - B$, is not statistically significant. Using the value $D - B < 0.13$ s^{-1} gives the following inequality:

$$k_{14} + K_{EQ}\left\{k_{13} + \frac{k_{15}{}^{M}[M] + k_{16} + k_{17}}{[O_2(^3\Sigma)]}\right\} < 1 \times 10^{-15}\ cm^3\ molecule^{-1}\ s^{-1}$$

Using this inequality, we can derive the upper bounds for a number of first-

TABLE 2

Rate coefficient data for $O_2(^1\Delta)$ behavior in the presence of I* and I

Process	*M*	*Rate coefficient* (cm^3 $molecule^{-1}$ s^{-1})	*Reference*
k_{-1}		$(2.7 \pm 0.3) \times 10^{-11}$	[18]
(k_1) [a]		$(7.8 \pm 0.8) \times 10^{-11}$ [a]	
k_{3a}		2.7×10^{-14} (1.3×10^3) [b]	[6, 16]
		8×10^{-14} (4×10^3) [b]	[8]
		1.1×10^{-13} (5.5×10^3) [b]	[19][c]
		8.4×10^{-14} (4.2×10^3) [b]	[19][c]
k_3		2.1×10^{-13}	This work
k_{eff} [d]		1.3×10^{-13}	[6]
		3×10^{-14}	[8]
		$<1 \times 10^{-15}$	This work
k_{13}		4.6×10^{-14}	[6]
		1×10^{-14}	[8]
		$<3.5 \times 10^{-16}$	This work
		$(0.9 \pm 4) \times 10^{-12}$	[18]
k_{14}		1.3×10^{-13}	[6]
		3×10^{-14}	[8]
		$<1 \times 10^{-15}$	This work
k_{15}	H_2O	$(2.5 \pm 0.5) \times 10^{-12}$	[20]
		$(2.1 \pm 0.3) \times 10^{-12}$	[21]
		1.7×10^{-12}	[17]
	$I(^2P_{3/2})$	$<1.7 \times 10^{-13}$	This work
		$<1.6 \times 10^{-14}$	[22]
k_{16}		<30 s^{-1} [e]	This work
k_{17}		<30 s^{-1}	This work
		7.8 s^{-1}	[23]

[a] The forward rate coefficient k_1 is determined by the reverse rate coefficient and the equilibrium constant K_{EQ}.
[b] The values in parentheses are the measured ratios of k_{3a}/k_{3b}.
[c] The quoted values were obtained in ref. 19 by alternative methods for calculating the iodine atoms in the system.
[d] The term k_{eff} is defined in the text as a combination of rate coefficients.
[e] The diffusion rate to the wall in this system is calculated to be 40 s^{-1} from the diffusion equation for a long cylinder and using a diffusion coefficient of 0.1 cm^2 s^{-1}.

order quenching processes that might be occurring in the COIL system. These rate coefficients are $k_{14} < 1 \times 10^{-15}$ cm^3 $molecule^{-1}$ s^{-1}, $k_{13} < 3.3 \times 10^{-16}$ cm^3 $molecule^{-1}$ s^{-1} ($k_{13} \ll k_{-1}$) and $k_{15}^{I} < 1.7 \times 10^{-13}$ cm^3 $molecule^{-1}$ s^{-1}. The rates $k_{16} < 30$ s^{-1} and $k_{17} < 30$ s^{-1} are determined as well. These upper bounds are considerably lower than those proposed by Derwent and Thrush [16] and are somewhat lower than those reported by Fisk and Hays

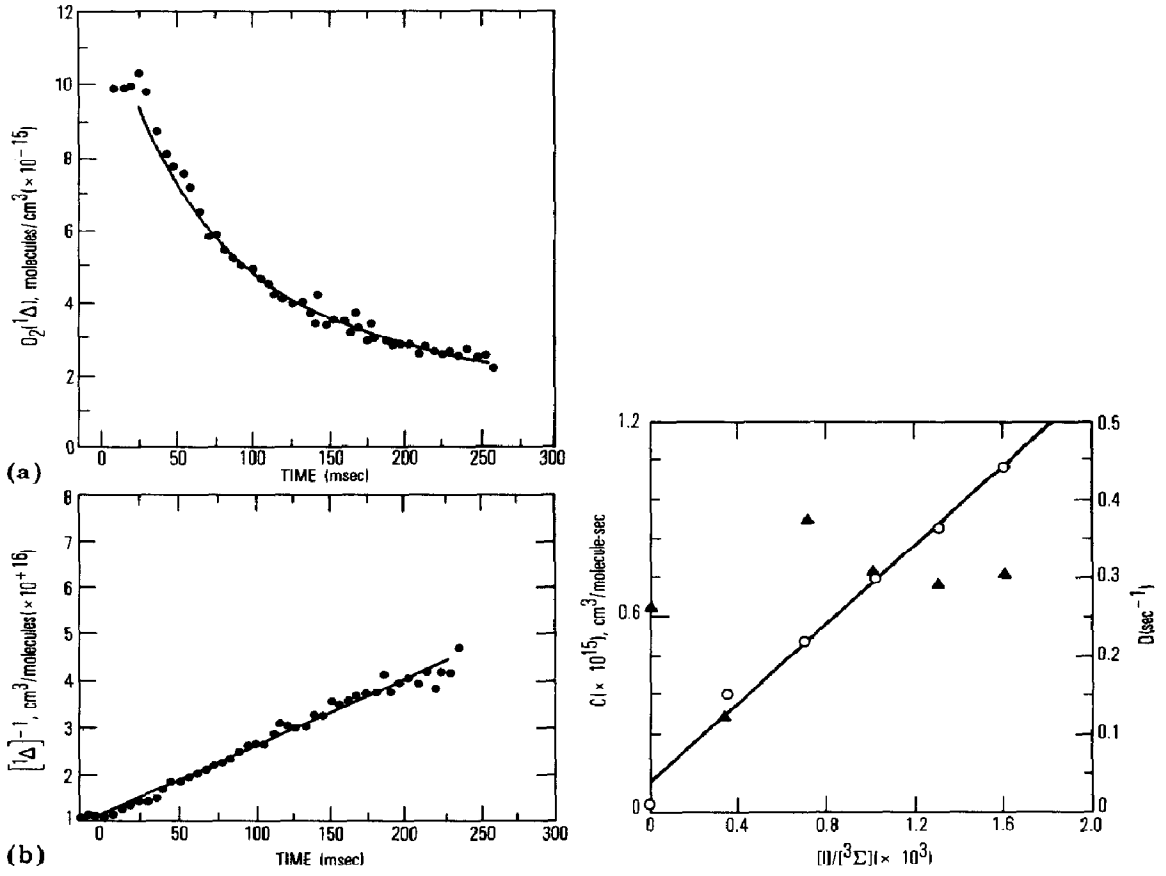

Fig. 5. (a) Decay of $O_2(^1\Delta)$ at high I* density ($[O_2(^1\Delta)]_0 = 1.0 \times 10^{16}$ molecules cm^{-3}; $[I_2]_0 = 1.98 \times 10^{13}$ molecules cm^{-3}): ——, fit to eqn. (12). (b) Data of (a) plotted as a pure second-order decay process.

Fig. 6. Plot of the first-order decay coefficient D (▲) and second-order decay coefficient C (○) as a function of $[I]/[O_2(^3\Sigma)]$ (see eqn. (12)).

[8]. The limit imposed on k_{17} is a factor of 4 larger than the accepted spontaneous emission rate from I* ($A_{ein} = 7.8$ s^{-1}) [23].

The results are offered as an example of the difficulty in deconvolving first- and second-order decays in a regime where their magnitudes are comparable. Although our results seem to be quite different from those of Fisk and Hays [8], it should be realized that they represent a difference in rate increase of 0.13 s^{-1} in one experiment and perhaps 2 s^{-1} in the other. Neither experiment should be considered to be definitive in determining these small changes in such a complex system. Clearly, the second-order component of the decay plays a significant role on the basis of independent evidence regarding the formation of $O_2(^1\Sigma)$. On the basis of our own work, we believe that most of the I-catalyzed *first-order* decay processes for $O_2(^1\Delta)$ can be ignored. The exceptions are the quenching processes for I*. The results of this study are compared with previous work in Table 2.

3.3. Decay of $O_2(^1\Delta)$ in the presence of I, I and I_2*

The stored energy in O_2^* is known to be capable of dissociating I_2. The efficiency of this dissociation process is thus a primary consideration for the design of a COIL device. Examination of the energy level diagram in Fig. 1 shows that two quanta of $O_2(^1\Delta)$ energy are required in order to break the I_2 bond (35.1 kcal mol^{-1}).

One of the original suggestions made by Ogryzlo and coworkers [24] and endorsed by the extensive work of Derwent and coworkers [25, 26] was that I_2 was both excited and dissociated by $O_2(^1\Sigma)$:

$$O_2(^1\Sigma) + I_2(X) \xrightarrow{k_{18a}} O_2(^3\Sigma) + 2I \tag{18a}$$

$$O_2(^1\Sigma) + I_2(X) \xrightarrow{k_{18b}} O_2(^3\Sigma) + I_2(A,A') \tag{18b}$$

$$O_2(^1\Delta) + I_2(A,A') \xrightarrow{k_{19a}} O_2(^3\Sigma) + I_2(B) \tag{19a}$$

$$O_2(^1\Delta) + I_2(A,A') \xrightarrow{k_{19b}} O_2(^3\Sigma) + 2I \tag{19b}$$

The $O_2(^1\Sigma)$ is formed by processes (3a) and (4). Although the details of the kinetic model that describes this mechanism are complex, the efficiency of the process in terms of $O_2(^1\Delta)$ storage molecules consumed can be written down by inspection relative to an efficiency of 1.0 for the consumption of two $O_2(^1\Delta)$ molecules per I_2 dissociated:

$$E = \frac{k_{18a}[I_2]}{k_{18}[I_2] + k_5^M[M] + k_6} \tag{20}$$

If I_2 is the chief loss mechanism for $O_2(^1\Sigma)$, then the dissociation efficiency is given by $E = k_{18a}/k_{18}$ which has been measured to be less than 0.2 [27]. If there are other loss mechanisms for $O_2(^1\Sigma)$, the efficiency is lower still.

Although this mechanism may be operative in the COIL system, recent experiments [17, 27] have shown that k_{18a} is too slow to account for the phenomenological dissociation rates of I_2 in O_2^*. A sequential excitation model [4] for I_2 dissociation can be proposed that is kinetically identical:

$$O_2(^1\Delta) + I_2(X) \xrightarrow{k_{21a}} O_2(^3\Sigma) + I_2^* \tag{21a}$$

$$I^* + I_2^* \xrightarrow{k_{21b}} 3I \tag{21b}$$

$$I^* + I_2(X) \xrightarrow{k_{22a}} I + I_2^* \tag{22a}$$

$$O_2(^1\Delta) + I_2^* \xrightarrow{k_{22b}} O_2(^3\Sigma) + 2I \tag{22b}$$

Either or both of the above sequences are kinetically acceptable; however, we prefer sequence (22) as it invokes collisions of the intermediate I_2^* with

a *majority* flow species ($O_2(^1\Delta)$) rather than a *minority* one (I^*). Either high vibrational levels of $I_2(X)$ or the electronically metastable $I_2(A,A')$ states have been examined as candidates for the intermediate state in processes (21) and (22). At present, there is qualitative support for all the suggested intermediate states. Further quantitative work must be done. Assuming that process (22) is responsible for the bulk of the I_2 dissociation, the efficiency of $O_2(^1\Delta)$ utilization is given by

$$E_{sq} = \frac{k_{22b}[O_2(^1\Delta)]}{R_{I_2^*}} \frac{k_{22a}[I_2]}{R_{I^*}} \tag{23}$$

where $R_{I_2^*}$ (s^{-1}) is the total rate of intermediate removal and R_{I^*} is the total rate of I^* removal. Thus, the overall dissociation efficiency is the product of the I^* utilization efficiency in process (22a) and the efficiency by which the I_2^* intermediate is used in process (22b). It is interesting to note that COIL devices work well at $[O_2(^1\Delta)]/[I_2]$ ratios of approximately 100 and that k_{22a}/k_3 is approximately 300. We believe that $k_{22b}[O_2(^1\Delta)]/R_{I_2^*}$ must be close to unity [4], although that may be an untenable assumption for a vibrationally excited $I_2(X)$ intermediate.

Removal of $O_2(^1\Delta)$ during the I_2 dissociation process is quite difficult to quantify experimentally. A seemingly trivial problem in flow tube methodology has rather serious consequences. It is difficult to mix small amounts of I_2 (molecular weight, 254) into a stream of O_2 (molecular weight, 32) in an efficient manner. A carrier gas (typically argon) is saturated with I_2 (0.1% - 10% I_2 in argon) and injected into the O_2 flow. We want to attain fast mixing and fast I_2 dissociation in order to decouple this $O_2(^1\Delta)$ loss from that caused by I and I^* (see Section 3.2). In order to achieve fast mixing (*i.e.* on the time scale of the I_2 dissociation), an Ar + I_2 mixture that represents roughly 5% of the O_2 molar flow rate must be injected. As shown schematically in Fig. 7, this argon then dilutes the O_2^* by 5% at the mixing point. In our system, it is impossible to measure an $O_2(^1\Delta)$ decrease due to I_2 dissociation of less than 2% in the presence of that dilution process. Table 3 is a matrix of percentage $[O_2(^1\Delta)]$ decrease as a function of the initial $[O_2(^1\Delta)]/[I_2]$ ratio and the mean dissociation efficiency. The entries resulting in greater than 20% loss of $O_2(^1\Delta)$ are omitted. The weak area of this method involves measuring efficiencies for large $[O_2(^1\Delta)]/[I_2]$ ratios. For ratios of 10^4, we are tempted to assign a 2% $O_2(^1\Delta)$ decrease to an efficiency of 0.01; however, that efficiency is properly expressed as 0.01 + 1.0 (−0.005).

Our own data are convincing for $[O_2(^1\Delta)]_0/[I_2]_0$ ratios of 100. They show that the dissociation efficiency is extremely high. We estimate that it is 0.75 ± 0.25 or that 3 ± 1 $O_2(^1\Delta)$ molecules are required to dissociate an I_2 molecule. Our results depend critically on the fact that the Halocarbon wax surface of the flow tube inhibits I recombination (and perhaps even I^* relaxation). Thus, I_2 is not *re-formed* on the walls by I recombination and *redissociated* by additional $O_2(^1\Delta)$. Results on $O_2(^1\Delta)$ loss in the I_2 dissocia-

TABLE 3

Fractional depletion of $O_2(^1\Delta)$ in the I_2 dissociation process

Mean dissociation efficiency E	*Fractional depletion for the following values of* $[O_2(^1\Delta)]_0/[I_2]_0$			
	10	10^2	10^3	10^4
1	0.2	0.02	2×10^{-3}	2×10^{-4}
0.1	—	0.2	0.02	2×10^{-3}
0.01	—	—	0.2	0.02
0.001	—	—	—	0.2

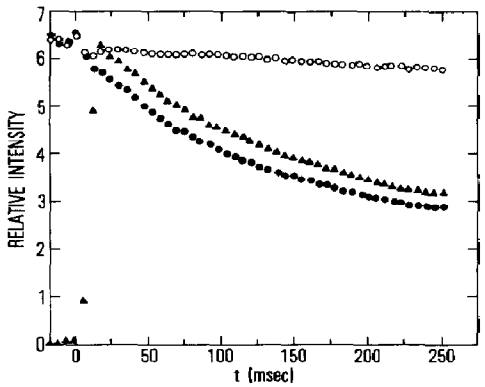

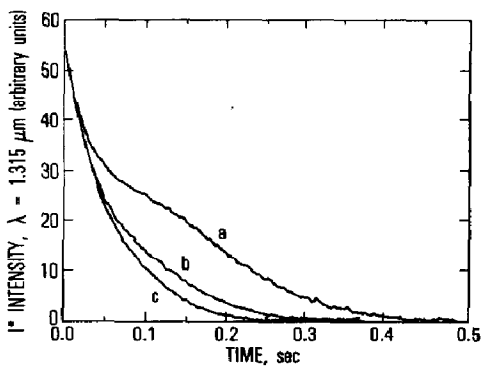

Fig. 7. Removal of $O_2(^1\Delta)$ during I_2 dissociation ($[O_2(^1\Delta)]/[O_2(^3\Sigma)] = 5.2 \times 10^{15}$ molecules $cm^{-3}/7.7 \times 10^{16}$ molecules cm^{-3}; $[I_2]_0 = 5.7 \times 10^{13}$ molecules cm^{-3} (●, ▲)): ○, dilution of $O_2(^1\Delta)$ by injected argon; ●, removal of $O_2(^1\Delta)$ by injected Ar + I_2; ▲, production of I* during I_2 dissociation.

Fig. 8. Normalized I* decay curves in O_2* in the presence of HI ($[O_2(^3\Sigma)] = 9.0 \times 10^{16}$ molecules cm^{-3}; $[O_2(^1\Delta)] = 7.9 \times 10^{15}$ molecules cm^{-3}; percentage photolysis of HI, 2.2%): curve a, $[HI]_0 = 6.4 \times 10^{14}$ molecules cm^{-3}; curve b, $[HI]_0 = 2.5 \times 10^{15}$ molecules cm^{-3}; curve c, $[HI]_0 = 4.4 \times 10^{15}$ molecules cm^{-3}.

tion regime clearly depend on the wall and the diffusional parameters of a particular experimental apparatus.

3.4. Extension to photoinitiated O_2–HI mixtures*

The decay of $O_2(^1\Delta)$ in time-resolved kinetics experiments can be monitored using the photodissociation of an I precursor in the apparatus shown in Fig. 3. Although $O_2(^1\Delta)$ is difficult to monitor directly in such experiments, [I*] which is proportional to it under the proper conditions (see eqn. (11)) can be monitored. The precursor chosen (HI) has an extremely small quenching coefficient for $O_2(^1\Delta)$. The results of these experiments are detailed in ref. 5. In the present context, we show the effect of increasing the density of the precursor (Fig. 8) in order to increase the initial I concentration produced by the laser. At low precursor densities, we have

shown that the coupled $I^*-O_2(^1\Delta)$ removal is dominated by a combination of *axial* diffusion, *radial* diffusion and cell pump-out. As the initial [I] + [I*] density increases, the removal does accelerate. We have shown that this acceleration is entirely consistent with process (3). Thus, we have independent confirmation that the first-order I-related loss processes for $O_2(^1\Delta)$ are extremely small.

4. Conclusion

In this paper the kinetic processes that remove $O_2(^1\Delta)$ in a COIL laser have been reviewed. In the absence of I_2, I* and I, the $O_2(^1\Delta)$ decays very slowly by energy pooling (second-order process (4)), gas phase quenching by H_2O and $O_2(^3\Sigma)$ and by wall quenching.

The removal of $O_2(^1\Delta)$ in the presence of I* and I is described by introducing the energy pooling of $O_2(^1\Delta)$ with I* (second-order process (3)) and several first-order quenching processes for $O_2(^1\Delta)$ and I*. In particular, we have considered the quenching of I* by H_2O, $O_2(^3\Sigma)$, I and the walls. These processes have an increasingly important effect on draining the $O_2(^1\Delta)$ storage reservoir as the $[I^*]/[O_2(^1\Delta)]$ ratio increases.

The presence of I_2 causes $O_2(^1\Delta)$ removal by more complex processes. The $O_2(^1\Delta)$ energy can be used by several mechanisms to break the I_2 bond and to create free I. The electronic equilibrium (process (1)) occurs rapidly, so that the I* density is determined by the $[O_2(^1\Delta)]/[O_2(^3\Sigma)]$ ratio and the total I density. The mechanism for I_2 dissociation by O_2^* is not completely defined; however, it certainly is represented by a *class* of processes that can be described as "chain reactions with chain branching". These include process (3a) followed by process (18a), process (21) and process (22). All these mechanisms consume two or more $O_2(^1\Delta)$ molecules per I_2 dissociated.

The use of $O_2(^1\Delta)$ to create the I laser medium can be avoided if an external power source is used to create free I. We have briefly described the use of excimer laser photolysis of HI to perform this function and to create the possibility of a repetitively pulsed version of the COIL laser.

Acknowledgments

I would like to thank my coworkers in the Aerophysics Laboratory: Dr. J. B. Koffend, Mr. G. I. Segal, Mr. C. E. Gardner, Mr. T. M. El-Sayed and Dr. J. V. V. Kasper. Many of the conclusions represent technical discussions over a number of years with Dr. H. V. Lilenfeld of McDonnell–Douglas Research Laboratory, Professor P. L. Houston and Professor J. R. Wiesenfeld of Cornell University and Dr. D. J. Benard and Dr. A. T. Pritt, Jr., of Rockwell Science Center. I would like to acknowledge gratefully both the

support of and consultation with the members of the Advanced Laser Branch of the Air Force Weapons Laboratory.

This work was supported by the Air Force Weapons Laboratory under U.S. Air Force Space Division Contract F04701-83-C-0084.

References

1 W. E. McDermott, N. R. Pchelkin, D. J. Benard and R. R. Bousek, *Appl. Phys. Lett.*, *32* (1978) 469.
2 D. J. Benard, W. E. McDermott, N. R. Pchelkin and R. R. Bousek, *Appl. Phys. Lett.*, *34* (1979) 40.
3 R. J. Richardson and C. E. Wiswall, *Appl. Phys. Lett.*, *35* (1979) 138.
4 R. F. Heidner III, C. E. Gardner, G. I. Segal and T. M. El-Sayed, *J. Phys. Chem.*, *87* (1983) 2348.
5 J. B. Koffend, C. E. Gardner and R. F. Heidner III, *J. Chem. Phys.*, *80* (1984) 1861.
6 R. G. Derwent and B. A. Thrush, *Trans. Faraday Soc.*, *67* (1971) 2036.
7 S. J. Arnold, M. Kubo and E. A. Ogryzlo, *Adv. Chem. Ser.*, *77* (1968) 133.
8 G. A. Fisk and G. N. Hays, *J. Chem. Phys.*, *77* (1982) 4965.
9 L. R. Martin, R. B. Cohen and J. F. Schatz, *Chem. Phys. Lett.*, *41* (1976) 394.
10 S. A. Lawton and A. V. Phelps, *J. Chem. Phys.*, *69* (1978) 1055.
11 K. H. Becker, W. Groth and U. Schurath, *Chem. Phys. Lett.*, *8* (1971) 259.
12 R. G. O. Thomas and B. A. Thrush, *J. Chem. Soc., Faraday Trans. II*, *71* (1975) 664.
13 R. G. Aviles, D. F. Muller and P. L. Houston, *Appl. Phys. Lett.*, *37* (1980) 358.
14 P. Borrell, P. M. Borrell and M. D. Pedley, *Chem. Phys. Lett.*, *51* (1977) 300.
15 A. Leiss, U. Schurath, K. H. Becker and E. H. Fink, *J. Photochem.*, *8* (1978) 211.
16 R. G. Derwent and B. A. Thrush, *Discuss. Faraday Soc.*, *53* (1972) 162.
17 R. F. Heidner III, C. E. Gardner, T. M. El-Sayed and G. I. Segal, *Chem. Phys. Lett.*, *81* (1981) 142.
18 A. T. Young and P. L. Houston, *J. Chem. Phys.*, *78* (1983) 2317.
19 R. F. Heidner III, C. E. Gardner, T. M. El-Sayed, G. I. Segal and J. V. V. Kasper, *J. Chem. Phys.*, *74* (1981) 5618.
20 D. H. Burde and R. A. McFarlane, *J. Chem. Phys.*, *64* (1976) 1850.
21 A. J. Grimley and P. L. Houston, *J. Chem. Phys.*, *69* (1978) 2339.
22 R. J. Donovan and D. Husain, *Trans. Faraday Soc.*, *62* (1966) 2023.
23 G. Brederlow, E. Fill and K. J. White, *The High Power Iodine Laser, Springer Ser. Opt. Sci.*, *34* (1983).
24 S. J. Arnold, N. Finlayson and E. A. Ogryzlo, *J. Chem. Phys.*, *44* (1966) 2529.
25 R. G. Derwent, D. R. Kearns and B. A. Thrush, *Chem. Phys. Lett.*, *6* (1970) 115.
26 R. G. Derwent and B. A. Thrush, *J. Chem. Soc., Faraday Trans. II*, *68* (1972) 720.
27 D. F. Muller, R. H. Young, P. L. Houston and J. R. Wiesenfeld, *Appl. Phys. Lett.*, *38* (1981) 404.